the plant journal

SEB Society for Experimental Biology

The Plant Journal (2019) **99,** 465–477 doi: 10.1111/tpj.14337

Extra-plastidial degradation of chlorophyll and photosystem I in tobacco leaves involving 'senescence-associated vacuoles'

Facundo M. Gomez[1,†], Cristian A. Carrión[1], María L. Costa[1], Christine Desel[2], Thomas Kieselbach[3], Christiane Funk[3], Karin Krupinska[2] and Juan Guiamet[1,*]

[1]*Instituto de Fisiología Vegetal, CONICET-Universidad Nacional de La Plata, cc 327, B1904DPS La Plata, Argentina,*
[2]*Botanisches Institut, Christian-Albrechts-Universität zu Kiel, 24098 Kiel, Germany, and*
[3]*Department of Chemistry, Umeå University, 90187 Umeå, Sweden*

Received 7 May 2018; revised 7 March 2019; accepted 14 March 2019; published online 15 April 2019.
*For correspondence (e-mail jguiamet@fcnym.unlp.edu.ar).
†Present address: AUSMA – UNComa, Q8370AQA, San Martin de los Andes, Argentina.

SUMMARY

Chlorophyll (Chl) loss is the main visible symptom of senescence in leaves. The initial steps of Chl degradation operate within the chloroplast, but the observation that 'senescence-associated vacuoles' (SAVs) contain Chl raises the question of whether SAVs might also contribute to Chl breakdown. Previous confocal microscope observations (Martínez *et al.*, 2008) showed many SAVs containing Chl. Isolated SAVs contained Chl *a* and *b* (with a Chl *a*/*b* ratio close to 5) and lower levels of chlorophyllide *a*. Pheophytin *a* and pheophorbide *a* were formed after the incubation of SAVs at 30°C in darkness, suggesting the presence of Chl-degrading activities in SAVs. Chl in SAVs was bound to a number of 'green bands'. In the most abundant green band of SAVs, Western blot analysis showed the presence of photosystem I (PSI) Chl-binding proteins, including the PsaA protein of the PSI reaction center and the apoproteins of the light-harvesting complexes (Lhca 1–4). This was confirmed by: (i) measurements of 77-K fluorescence emission spectra showing a single emission peak at around 730 nm in SAVs; (ii) mass spectrometry of the most prominent green band with the slowest electrophoretic mobility; and (iii) immunofluorescence detection of PsaA in SAVs observed through confocal microscopy. Incubation of SAVs at 30°C in darkness caused a steady decrease in PsaA levels. Overall, these results indicate that SAVs may be involved in the degradation of PSI proteins and their associated chlorophylls during the senescence of leaves.

Keywords: senescence-associated vacuoles, photosystem I, chlorophyll degradation, tobacco, *Nicotiana tabacum*.

INTRODUCTION

Chlorophyll (Chl) loss is a distinctive feature of leaf senescence, as well as a convenient marker of chloroplast degradation (Krupinska, 2007; Ougham *et al.*, 2008). Unlike the degradation of proteins, which provides N for remobilization to other parts of the plant, chlorophyll is degraded into N-containing catabolites that are eventually stored in the central vacuole in a non-remobilizable form (Hörtensteiner, 2006; Kuai *et al.*, 2018). Thus, it is assumed that the chlorophyll degradation pathway has evolved as a detoxification process to avoid the potential risk of phototoxicity that might arise as a consequence of the dismantling of Chl–protein complexes and the release of free Chl or photodynamic Chl catabolites (Mach *et al.*, 2001; Pruzinska *et al.*, 2003; Li *et al.*, 2017).

There is strong evidence for the operation of a chlorophyll degradation pathway that involves a series of reactions taking place in the chloroplast and cytosol, with the eventual disposal of final chlorophyll catabolites in the central vacuole. The initial steps of chlorophyll breakdown occur in the chloroplast and are catalyzed by chloroplast enzymes (Hörtensteiner, 2006). First, the Chl–protein complexes of the thylakoid membranes are dismantled. Then, Chl *a* is converted into pheophytin *a* by Mg-dechelatase (the product of the *SGR* gene) and then pheophytin *a* is dephytilated by pheophytinase to yield pheophorbide *a* (Schelbert *et al.*, 2009; Guyer *et al.*, 2014; Kuai *et al.*, 2018). Oxygenolytic cleavage of the porphyrin ring by pheophorbide oxygenase results in the formation of the first colorless chlorophyll catabolites (Pruzinska *et al.*, 2003; Hörtensteiner, 2006); fluorescent and non-fluorescent chlorophyll catabolites are eventually disposed in the central vacuole (Hinder *et al.*, 1996; Kuai *et al.*, 2018). There is

no separate pathway for the degradation of Chl *b*, which is broken down through this same pathway after conversion into Chl *a* by Chl *b* reductase and 7-hydroxymethyl chlorophyll *a* reductase (Scheumann *et al.*, 1999; Sato *et al.*, 2009; Meguro *et al.*, 2011). Although for a long time chlorophyllase was thought to catalyze the first reaction of chlorophyll degradation in senescing leaves, current evidence shows that it has no role during senescence (Schenk *et al.*, 2007) or during chlorophyll turnover in Arabidopsis seedlings subjected to heat shock (Lin *et al.*, 2014). Instead, chlorophyllase participates in defense against necrotrophic bacteria (Kariola *et al.*, 2005) and chewing insects (Hu *et al.*, 2015). Chlorophyll dephytilase, another enzyme catalysing the removal of the phytol side chain of chlorophyll, is not expressed in senescing leaves (Lin *et al.*, 2016).

Lytic vacuoles with high protease activity ('senescence-associated vacuoles') accumulate in senescing leaves of soybean [*Glycine max* (L.) Merril] and *Arabidopsis thaliana* (Otegui *et al.*, 2005). Other extra-chloroplastic structures containing plastid components have also been observed in senescing leaves (Chiba *et al.*, 2003; Ishida *et al.*, 2008; Wada *et al.*, 2009; Michaeli *et al.*, 2014; Wang and Blumwald, 2014). 'Senescence-associated vacuoles' (SAVs) are small (0.5–0.8 μm diameter) and clearly distinguishable from the central vacuole because they are more acidic and have different protein markers in their limiting membrane (Otegui *et al.*, 2005). Confocal microscopy observations and biochemical analysis of isolated SAVs have shown that they contain proteins of the chloroplast stroma, and that they can break down Rubisco *in vitro* (Martínez *et al.*, 2008; Carrión *et al.*, 2013). This suggests that SAVs play a role in the degradation of stromal proteins of the chloroplast. Consistently, some SAVs also showed a fluorescence signal with an emission spectrum similar to the chlorophyll fluorescence signal from the chloroplasts, and isolation of SAVs allowed us to show that Chl *a* is present in SAVs (Martínez *et al.*, 2008). Thus, it is tempting to suggest that a fraction of leaf chlorophyll might be broken down within SAVs. Therefore, the main goals of this work were to determine: (i) the pigment composition of SAVs; (ii) whether the chlorophyll in SAVs is bound to specific Chl-binding proteins; and (iii) whether Chl and Chl-binding proteins can be broken down within SAVs.

RESULTS

Chlorophyll and Chl degradation in SAVs

Confocal microscopy observations of live cells isolated from senescing leaves showed that some SAVs (detected by staining with the acidotropic marker Lysotracker Red) contained a clear fluorescence signal corresponding to chlorophyll (Figure 3b in Martínez *et al.*, 2008). To examine their pigment composition, SAVs from leaves senescing in darkness were isolated and partially purified by sucrose density centrifugation. We have previously employed this protocol and shown that it yields SAVs with no contamination by chloroplasts or the central vacuole (Martínez *et al.*, 2008). To confirm that Chl in this fraction is actually confined within SAVs, we ran a flow cytometry analysis of isolated SAVs stained with the acidotropic marker Neutral Red (which is similar to Lysotracker Red and labels SAVs *in vivo*; Otegui *et al.*, 2005) or with R6502, a fluorescent probe for cysteine protease activity (Carrión *et al.*, 2013). Figure 1 shows that most (approximately 59%) of the vesicles in the SAV-enriched fraction fluoresced simultaneously in the chlorophyll and Neutral Red channels (compare Figure 1a with c): that is, most of the Chl detected in this fraction was contained within acidic SAVs stained by Neutral Red. Likewise, many Chl-containing vesicles also contained high cysteine protease activity detected with R6502 (compare Figure 1b with d). There were events in the flow cytometry analysis that had a Chl signal with virtually no Neutral Red fluorescence (Figure 1a), thus raising the possibility of the contamination of isolated SAVs by chloroplasts or chloroplast fragments. Western blots performed at each step of the SAV isolation protocol show an enrichment of V-pyrophosphatase, a marker of SAVs (Otegui *et al.*, 2005), in the SAV fraction recovered after the first and second ultracentrifugation steps (Figure 1e), whereas the D1 protein of chloroplasts disappears completely after the first centrifugation step of 3000 ***g***, intended to pull down chloroplasts and chloroplast fragments (Figure 1f). Overall, this rules out the possibility that Chl in the SAV fraction represented an artifact of the isolation procedure or contamination by chloroplast fragments. The occurrence of events with chlorophyll fluorescence signal without, for example, Neutral Red fluorescence may reflect incomplete staining by Neutral Red or quenching of weak Neutral Red fluorescence signals by chlorophyll.

The HPLC analysis of the pigment composition of isolated SAVs showed two major peaks corresponding to Chl *a* and Chl *b* (Figure 2). Spectrophotometric measurements of SAVs dissolved in buffered 80% acetone using the equations derived by Sims and Gamon (2002) indicated that their Chl *a*/*b* ratio was 5.12 ± 1.01 (mean $\pm$ SD), which is significantly higher than the Chl *a*/*b* ratio that is typical of leaves (3.00 ± 0.08) or thylakoids. Levels of chlorophyllide *a* (Chlide *a*) or pheophytin *a* (Phein *a*) were much lower than those of Chl, whereas pheophorbide *a* (Pheide *a*) was not detected (Figure 2). To determine whether Chlide *a*, Phein *a*, Pheide *a* and/or other early Chl catabolites can be formed within SAVs, isolated SAVs were incubated *in vitro* to follow the changes in pigment composition. *In vitro* incubation of isolated SAVs in darkness initially caused a substantial increase in the levels of Chlide *a* and the appearance of detectable levels of Pheide *a* and Phein *a* (Figure 3). For example, the levels

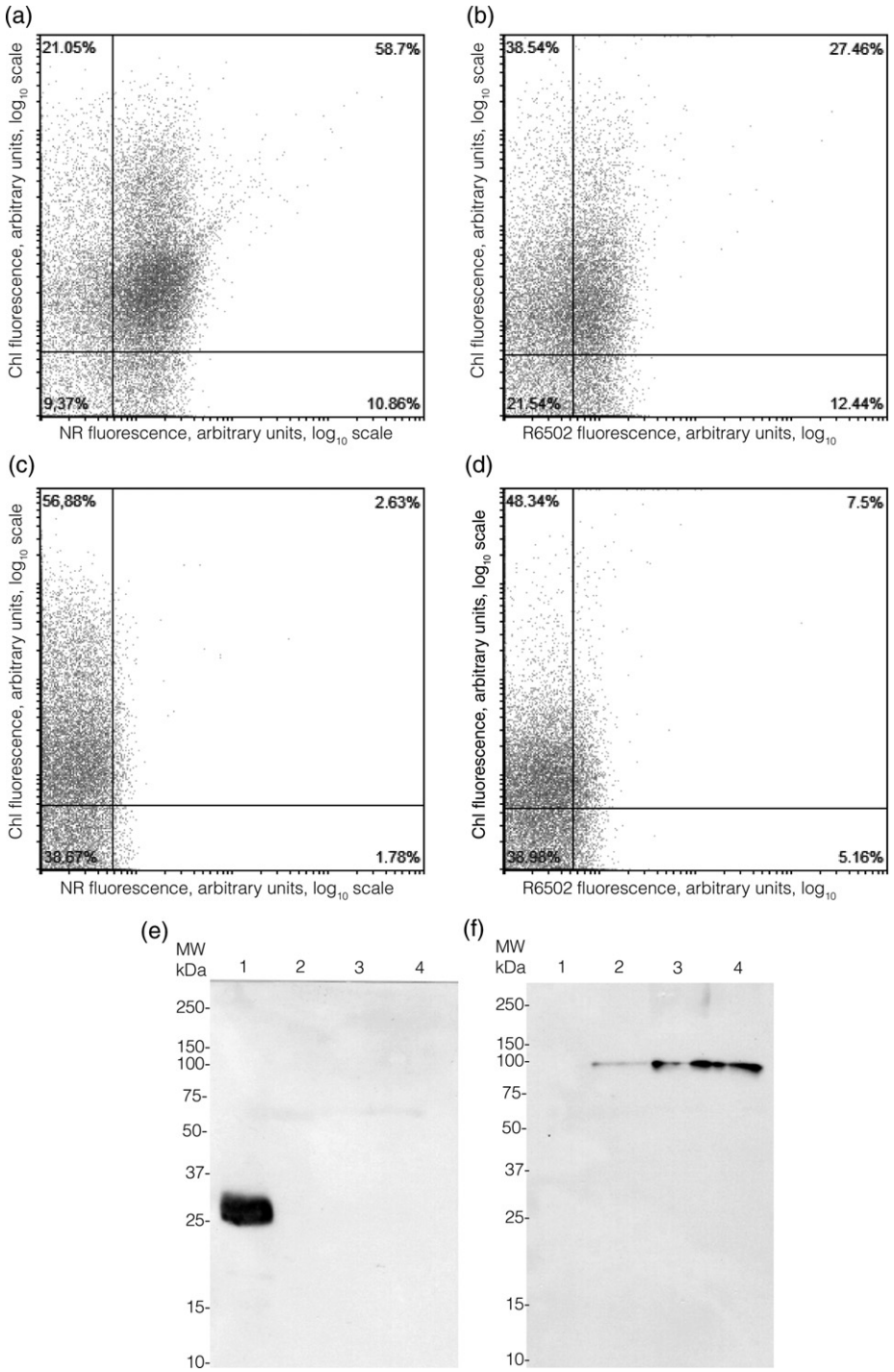

Figure 1. (a–d) Flow cytometry analysis of isolated 'senescence-associated vacuoles' (SAVs). Density plots of SAVs analysed by fluorescence in the chlorophyll (Chl) and Neutral Red (NR) channels (panels a and c), or in the Chl and R6502 channels (panels b and d). Isolated SAVs were incubated with NR (a) or R6502 (b) before analysis, or were left unstained as controls (c and d). For each panel, 20 000 events were gated. Percentage values in the corners of each figure represent the percentage of events within the thresholds marked by vertical and horizontal lines. Panels e and f show Western blots of SAVs probed with anti-D1 (e) and anti-V-pyrophosphatase (f) antibodies. Lanes: 1, crude extract; 2, post-3000 ***g*** supernatant; 3, SAVs isolated after one ultracentrifugation step; 4, SAVs isolated after the second ultracentrifugation step. SAVs corresponding to lane 4 were used for all subsequent analysis. Lanes were loaded with equal volumes of each fraction.

of Chlide *a* increased about fivefold during the first 6 h of incubation. The levels of Pheide *a* and Phein *a* also began to increase significantly during the incubation of isolated SAVs, but not as early as the levels of Chlide *a*. The levels of Chlide *a* remained relatively constant after 6 h of incubation, however, whereas the levels of Phein *a* and

Pheide *a* continued to increase up to 14 h of incubation. Thus, SAVs contained chlorophyll, and they also appeared to be competent for Chl degradation to yield early chlorophyll catabolites, i.e. Phein *a* and Pheide *a.*

Identification of Chl-binding proteins in SAVs

In the thylakoid membranes of chloroplasts, Chl is bound to specific proteins to form Chl–protein complexes (Scheer, 2006), and there are presumably no significant levels of free Chl in living cells. Therefore, we attempted to determine whether Chl is bound to specific Chl-binding proteins in SAVs. Proteins from isolated SAVs were solubilized with a mixture of mild detergents (see Experimental procedures) and separated by non-denaturing gel electrophoresis to preserve Chl–protein interactions and resolve Chl–protein complexes (Sárvári and Nyitrai, 1994). With thylakoid membrane samples, this electrophoresis system separated a number of 'green bands' (i.e. Chl–protein complexes), with almost no release of free Chl (Figure 4a). A few 'green bands' were separated from isolated SAVs. Most of the Chl in SAVs appeared to be bound to a band with a slower electrophoretic mobility than any other 'green band' from SAVs or thylakoids. Also, this slow mobility band was clearly specific to SAVs, and no green band of similar mobility was seen in thylakoids. When examined under UV illumination, faster migrating bands fluoresced strongly (Figure 4b), whereas bands with slow mobility did not, which is consistent with the photochemical quenching of fluorescence in the photosystem I (PSI) reaction center (e.g. Allen and Staehelin, 1991). MS/MS analysis for this slow migrating Chl–protein complex indicated that it contained PSI proteins, plus stromal enzymes

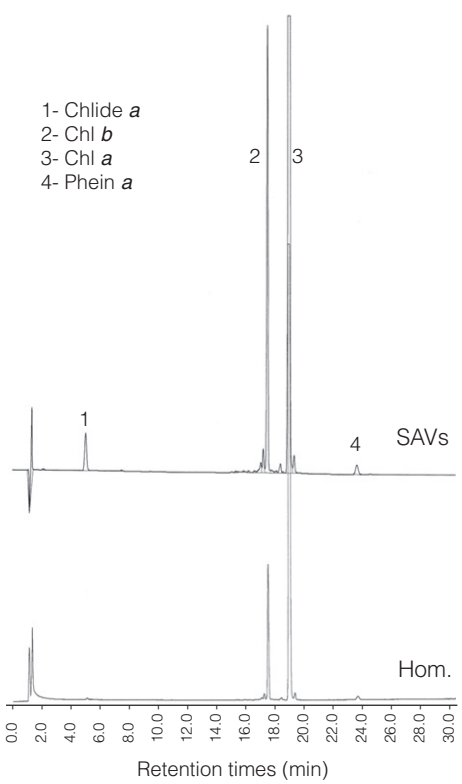

Figure 2. HPLC chromatograms of pigments extracted from 'senescence-associated vacuoles' (SAVs) and detected by absorbance at 667 nm. Upper panel: chromatogram from freshly isolated SAVs. Lower panel: chromatogram of the homogenized leaf tissue from which the SAVs were isolated. Peaks corresponding to the retention times of standards are marked: 1, chlorophyllide *a* (Chlide *a*); 2, chlorophyll *b* (Chl *b*); 3, chlorophyll *a* (Chl *a*); and 4, pheophytin *a* (Phein *a*). Retention times are shown along the *x*-axis. For the retention times of standards, see Figure S1.

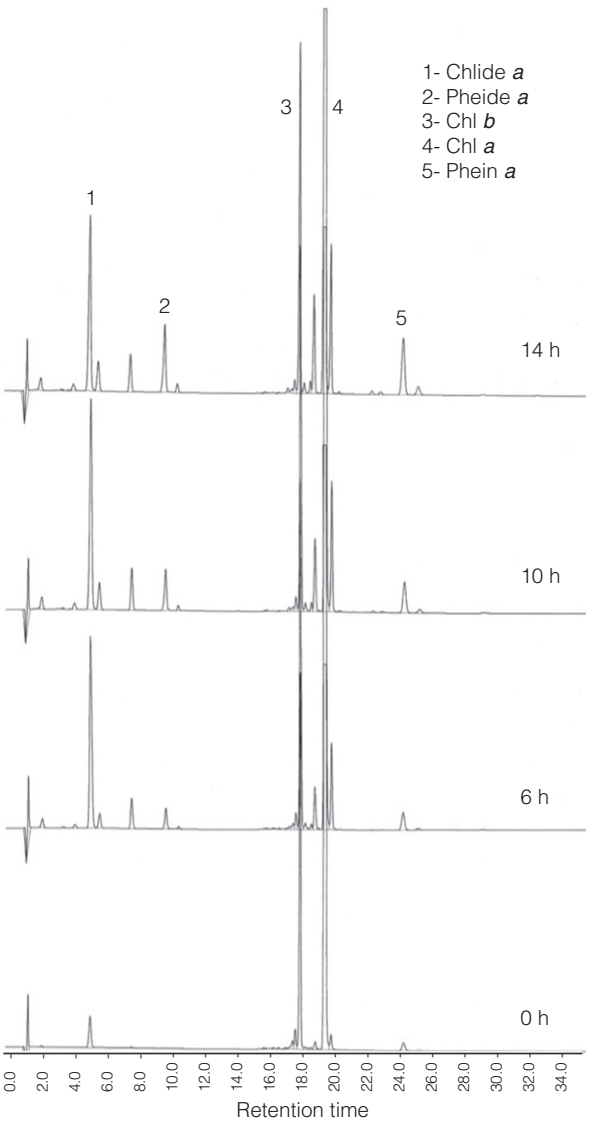

Figure 3. HPLC chromatograms of pigments extracted from 'senescence-associated vacuoles' (SAVs) incubated in darkness at 30°C for 6, 10 and 14 h, and detected at 667 nm. Peaks corresponding to the retention times of standards are marked: 1, chlorophyllide *a* (Chlide *a*); 2, pheophorbide *a* (Pheide *a*); 3, chlorophyll *b* (Chl *b*); 4, chlorophyll *a* (Chl *a*); and 5, pheophytin *a* (Phein *a*). Numbers below the peaks represent retention times.

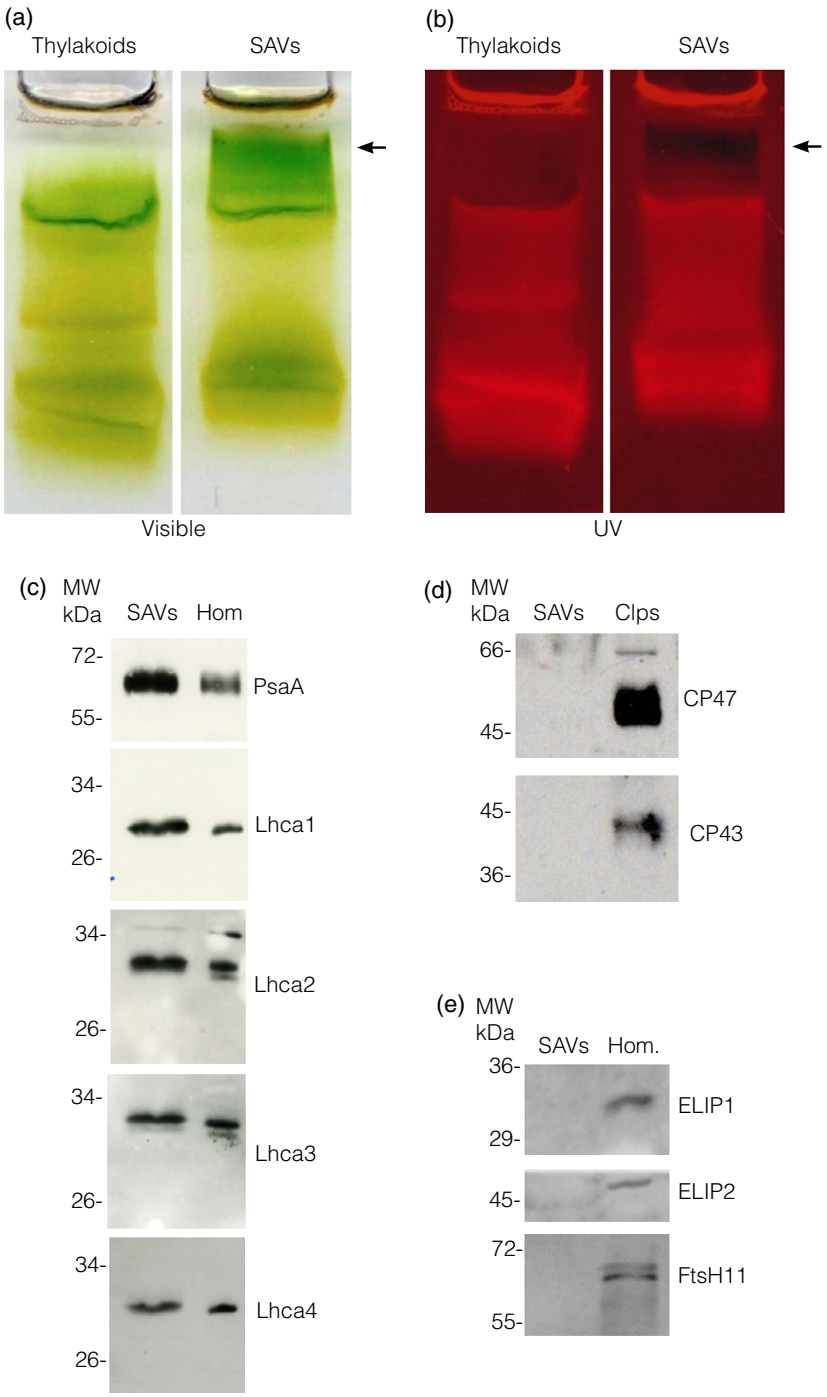

Figure 4. Detection of photosystem I (PSI) proteins in 'senescence-associated vacuoles' (SAVs) from tobacco leaves. (a, b) Non-denaturing gel electrophoresis of isolated SAVs and thylakoids, illuminated with visible (a) or UV light (b). An aliquot of solubilized sample equivalent to 14 μg of chlorophyll (Chl) was loaded in each lane. The arrows show the green band, quenched under UV light, that was subjected to MS/MS identification. (c) Western blot analysis of the leaf homogenate (Hom) and isolated SAVs from tobacco leaves senescing in darkness for 2 days revealed antibodies against PSI proteins. The equivalent to 1.1 μg of Chl was loaded per lane. (d) Western blot analysis of CP43 and CP47 (PSII) in senescing chloroplasts (Clp, the *3500 **g*** pellet from the SAV isolation protocol) compared against SAVs purified by two ultracentrifugation steps. (e) Western blot analysis of ELIP1, ELIP2 and FtsH11 in SAVs and homogenate leaf extract (Hom). A 7.5-μg portion of protein was loaded per lane for the Western assays shown in (d) and (e). Leaves incubated in darkness for 2 days before the isolation of SAVs. The position of apparent molecular mass markers is shown on the left-hand side of each blot.

of the Calvin cycle and subunits of chloroplastic ATP synthase, as well as vacuolar H^+-ATPases that probably co-migrated with PSI proteins in our electrophoresis system (Table 1). To confirm the presence of PSI proteins, which in our green gel system appear to bind a large part of the Chl in SAVs, isolated SAVs were subjected to sodium dodecyl sulfate polyacrylamide gel electrophoresis (SDS-PAGE) and Western blot analysis with specific antibodies. The PSI core protein PsaA and the light-harvesting antenna proteins Lhca1, Lhca2, Lhca3 and Lhca4 were detected in SAVs isolated from leaves senescing in darkness for 2 days (with a Chl loss of 3.0 SPAD units; Figure 4c). Some of these proteins (e.g. PsaA, Lhca1 and Lhca4) were enriched in the SAV fraction as compared with a crude leaf homogenate (Hom). Thus, the Chl in SAVs is largely bound to Chl-binding proteins of PSI.

Table 1 Mass spectrometric identification of proteins in band 1 excised from green gels (arrowed band). GI number, description, Mascot score, predicted mass, number of peptides matched, and percentage of sequence coverage

Sample Accession	Description	Mascot score	Precursor mass [Da]	Peptides matched	Sequence coverage [%]
Green band 1					
gi|2499964	PsaB subunit of photosystem I reaction center [*Antirrhinum majus* L.]	623	82 368	21	8
gi|131167	PsaD subunit of photosystem I reaction center [*Nicotiana sylvestris* Speg. & Comes]	553	22 410	15	36.8
gi|397555	PsaH subunit of photosystem I reaction center [*Nicotiana sylvestris* Speg. & Comes]	287	15 328	9	30.3
gi|3914442	PsaH subunit of photosystem I reaction center [*Brassica rapa* L. ssp. *rapa*]	261	15 400	7	30.3
gi|407769	PsaDb subunit of photosystem I reaction center [*Nicotiana sylvestris* Speg. & Comes]	258	23 441	9	32.2
gi|1217601	PsaEb subunit of photosystem I reaction center [*Nicotiana sylvestris* Speg. & Comes]	253	15 599	5	44.2
gi|29468504	PsaL subunit of photosystem I reaction center [*Nicotiana attenuata* Torr. ex S. Watson]	230	23 256	8	32.7
gi|2499966	PsaEa subunit of photosystem I reaction center [*Nicotiana sylvestris* Speg. & Comes]	224	15 090	6	31.9
gi|401322	A catalytic subunit of V-type H^+ ATPase [*Gossypium hirsutum* L.]	201	68 479	5	10.4
gi|255560497	β subunit of vacuolar ATP synthase, putative [*Ricinus communis* L.]	194	45 499	5	14.5
gi|168812218	Chlorophyll *a*/*b* binding protein type I, putative [*Cupressus sempervirens* L.]	162	14 298	2	17.2
gi|3687676	RuBisCO activase precursor, fragment [*Datisca glomerata* (Presl) Baill]	159	26 933	3	14.8
gi|115792	Chlorophyll *a*/*b* binding protein 21, LHCII type I CAB21 [*Nicotiana tabacum* L.]	150	28 108	2	13.2
gi|68139361	β subunit of chloroplastic ATP synthase [*Alisma plantago-aquatica* L.]	143	48 593	3	12.2
gi|12004115	β subunit of chloroplastic ATP synthase [*Douglasia nivalis* Lindl.]	139	52 382	3	6.8

Previously, we failed to detect the D1 and LHCII proteins of PSII by the Western blotting of isolated SAVs (Martínez *et al.*, 2008). We further explored the presence of other thylakoid proteins in SAVs through SDS-PAGE and Western blot analysis. The CP43 and CP47 proteins of PSII were undetectable in SAVs (Figure 4e), thus confirming the absence of PSII proteins that we reported previously (Martínez *et al.*, 2008). We also failed to detect other chloroplastic proteins, i.e. ELIP1, ELIP2 and FtsH11 (Figure 4e), in isolated SAVs.

Photosystem-I fluorescence in SAVs

To further test for the presence of PSI components in SAVs, we analyzed the fluorescence emission spectra of SAVs at room temperature (20–22°C) and at low temperature, i.e. 77 K (Figure 5). At room temperature, the emission spectra of SAVs and that of the crude homogenate from which SAVs were isolated (and which represents mostly the fluorescence from thylakoids) were very similar (Figure 5a). This is consistent with the observation that the fluorescence emission spectra of chloroplasts and SAVs measured by confocal microscopy *in vivo* at room temperature are almost identical (Martínez *et al.*, 2008). When the fluorescence emission spectrum of the crude homogenate was instead recorded at low temperature (77 K; Figure 5b), two major emission peaks around 680 and 730 nm, representing emission from PSII and PSI, respectively, were obtained (Govindjee, 2004). Strikingly, in isolated SAVs only the 730-nm fluorescence emission peak derived from PSI was observed (Figure 5b). Moreover, at room temperature SAVs showed changes in absorbance at 830 nm typical of PSI activity, i.e. P700 reduction/oxidation (Schreiber, 2004). Figure 6 shows typical increases in absorbance at 830 nm that represent P700 oxidation after irradiation with far-red light. Clearly, there are functional PSI centers in both the crude leaf homogenate and the SAVs. The crude leaf homogenate also displays typical variable fluorescence as a result of PSII oxidation/reduction, whereas no variable fluorescence associated with PSII could be detected in SAVs (Figure 6, lower panel). All this evidence indicates that SAVs contain PSI units, but possibly no more than traces of PSII.

Immunolocalization of PsaA in SAVs

Cells isolated from senescing leaves (i.e. leaves incubated for 2 days in darkness) were probed with an anti-PsaA antibody (Figure 7). The SAG12-GFP fluorescence signal labels SAVs (Otegui *et al.*, 2005; Carrión *et al.*, 2013). i.e. the small, round, acidic structures located outside the plastids (Figure 7). Many SAVs were also labelled by Alexa Fluor

546, implying that they contain the PsaA protein of PSI. Alexa Fluor labelling was specific, as there was virtually no signal in the 560–590 nm range in the negative control samples. Arrows show several SAVs where Chl, SAG12-GFP and the Alexa Fluor 546 signal representing PsaA inmunodetection were colocalized (linear Pearson coefficient equal to 0.74 ± 0.02 standard error, non-linear Spearman's rank correlation coefficient equal to 0.64 ± 0.04; French *et al.*, 2008), confirming that Chl is associated with PSI proteins in SAVs. It should be noted that, as expected, the anti-PsaA also labels chloroplasts, and some SAG12-GFP signal appears around chloroplasts, apparently in their periphery, as we have already noted in tobacco (*Nicotiana tabacum* L.) (Carrión *et al.*, 2013).

Degradation of the PsaA Chl-binding protein of PSI within isolated SAVs

The SAVs form a lytic compartment within senescing leaf cells with very intense proteolytic activity (Otegui *et al.*, 2005), and isolated SAVs can degrade Rubisco (Martínez *et al.*, 2008; Carrión *et al.*, 2013), and presumably other stromal proteins, *in vitro*. This raises the question of whether SAVs can also degrade PSI proteins. The incubation of isolated SAVs at 30°C in darkness resulted in a rapid decrease in the levels of the PsaA Chl-binding protein of the PSI reaction center (Figure 8). These data clearly show that SAVs are active in the degradation of the PSI proteins contained within these vacuoles.

DISCUSSION

Purity of the SAV fraction isolated by ultracentrifugation

Some of the findings of this work depend critically on the purity of the isolated SAVs, and on whether this fraction might be contaminated by chloroplasts or chloroplast fractions. The purity of the SAV fraction isolated by the method described here has been tested in a previous paper (Martínez *et al.*, 2008), and more specifically the absence of chloroplast contamination is confirmed here by the enrichment of V-pyrophosphatase and the complete absence of the D1 protein of PSII (Figure 1e,f) in isolated SAVs. Several other findings in this work rule out contamination by chloroplast fragments, including: (i) the very high chl *a*/*b* ratio of SAVs; (ii) the lack of photosystem-II proteins; (iii) the lack of PSII low-temperature signals; and (iv) the lack of PSII variable fluorescence. Thus, we rule out the possibility that the chlorophyll and PSI proteins found in SAVs represent an artefact of the isolation procedure.

Senescence-associated vacuoles

In recent years, evidence has accumulated for the presence of chloroplast proteins in vesicular structures outside the chloroplasts of senescing leaves (Chiba *et al.*, 2003; Ishida *et al.*, 2008; Martínez *et al.*, 2008; Wada *et al.*, 2009; Carrión *et al.*, 2014; Michaeli *et al.*, 2014; Wang and Blumwald, 2014). 'Senescence-associated vacuoles', 'Rubisco-containing bodies' (RCBs), 'ATI-PS' vesicles and 'CV-containing vesicles' (CCVs) are detected in senescing cells, and they contain chloroplast proteins. The limited information available about SAVs and RCBs suggest a number of apparent differences: for example, the acid milieu and high peptidase activity of SAVs (Otegui *et al.*, 2005), and the lack of Chl in RCBs (Ishida *et al.*, 2008). In addition to chloroplast proteins, SAVs contain components presumably trafficking through the secretory pathway (e.g. SAG12 and V-type H^+ PPAse). The observation of RCBs is routinely enhanced by the blockage of V-type H^+ ATPase with concanamycin A on the assumption that this treatment brings the vacuolar pH closer to neutrality, thus reducing vacuolar degradation of RCB contents, and allowing for RCB detection through fluorescence of reporter proteins initially targeted to chloroplasts (Ishida *et al.*, 2008). Concanamycin A might interfere with trafficking through the trans-Golgi network (Dettmer *et al.*, 2006), however, thereby putatively depleting SAVs of components coming through the secretory pathway. In fact, SAG12-GFP becomes undetectable and peptidase activity is abolished in SAVs of leaves treated with concanamycin A (Carrión *et al.*, 2014). This complicates the potential detection of SAVs and RCBs simultaneously in the same cells. Thus, SAVs and RCBs might represent different structures visualized under different experimental conditions, both possibly involved in stromal protein degradation (Ishida *et al.*, 2008; Carrión *et al.*, 2014). CCVs are devoid of chlorophyll and SAG12 (Wang and Blumwald, 2014), suggesting that they are different from SAVs. ATI-PS is yet another vesicular structure found in senescing leaves, apparently similar to SAVs in that it contains stromal proteins and chlorophyll (Michaeli *et al.*, 2014). The ATI protein interacts with a number of thylakoid proteins, including LHCA4, and analysis of knock-down lines shows that it may be involved in the degradation of chloroplast peroxyredoxin. A systematic analysis of extraplastidial vesicles (i.e. SAVs, RCBs, CCVs and ATI-PS) containing chloroplast proteins in senescing leaves should be undertaken to improve our understanding of the possible interrelations between these vesicles, their specific functions and whether they represent different pathways, or the same structure probed through different approaches or at different stages during senescence.

The observations that stromal proteins are relocated to SAVs in senescing leaves (Martínez *et al.*, 2008) and that SAVs apparently contain the highest levels of cysteine protease activity of senescing leaf cells (Otegui *et al.*, 2005) indicate that SAVs may play a role in chloroplast stromal protein degradation during senescence. The data presented here also suggest a role for SAVs in the degradation of PSI proteins and their associated chlorophylls.

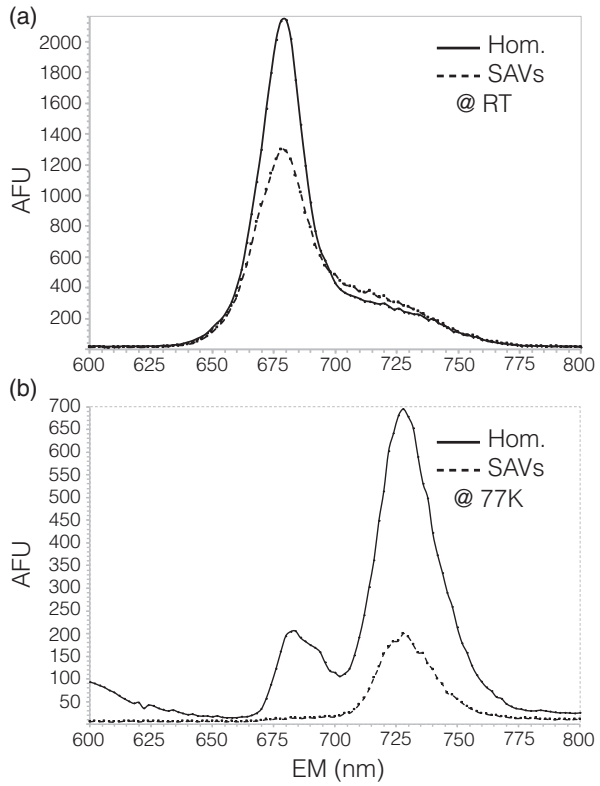

Figure 5. Room temperature (a) and 77-K (b) fluorescence emission spectra of 'senescence-associated vacuoles' (SAVs) and the crude leaf homogenate (Hom) from which SAVs were isolated. Leaves were induced to senesce in darkness for 2 days, and the emission spectra were measured with excitation at 440 nm. The concentrations of chlorophyll (Chl) for these measurements were 6.7 (crude leaf homogenate) and 16 (SAVs) μg Chl ml^{-1}. Previous assays showed that self-absorption was negligible at these concentrations of chlorophyll. AFU, arbitrary fluorescence units; EM, emission wavelength.

Photosystem I in isolated SAVs

Various lines of evidence (i.e. immunological analysis, mass spectrometry, fluorescence emission spectra and P700 oxidation) show that the Chl in SAVs is mainly bound to PSI apoproteins. Consistent with the high proteolytic activity of SAVs, we have found that the PsaA protein, one of the PSI core proteins, can be degraded within these vacuoles.

Thus, SAVs might be involved specifically in PSI degradation, and this raises a question about the sorting mechanism(s) that might specifically direct PSI to SAVs. Two important, unresolved points concern the trafficking mechanism re-locating PSI to SAVs, and whether PSI proteins in SAVs are aggregated, are soluble in a water milieu or are bound to lamella-like membrane structures. In thylakoid membranes of barley (*Hordeum vulgare* L.), a fraction of PSI is present in an oligomeric form running more slowly than the major PSI band in non-denaturing gels (Preiss *et al.*, 1993), which is similar to the slow mobility of the green band containing PsaA of SAVs in our non-denaturing gels (Figure 4a). Although the mechanism for transport of chloroplast proteins outside the plastid is presently unknown, is has been recently shown that the CCV protein is responsible for vesicle release from the chloroplasts of plants under stress conditions (Wang and Blumwald, 2014).

Isolated SAVs can digest PSI proteins contained therein, which is also consistent with the high peptidase activity detection *in vivo* in SAVs using a fluorogenic substrate (Carrión *et al.*, 2013). Although our data show that PSI proteins can be degraded in SAVs, we cannot estimate quantitatively the proportion of PSI complexes or chlorophyll molecules that may be broken down through this route to assess the importance of SAVs for PSI degradation during senescence.

Chl degradation in SAVs

The chlorophyll degradation pathway consists of a series of reactions leading to the production of colorless catabolites that are stored in the central vacuole (Hörtensteiner, 2006). This pathway may be initiated by the disassembly of the Chl–protein complexes of thylakoid membranes (Hörtensteiner, 2009). Free chlorophyll is then converted to Phein *a* by Mg^{2+}-dechelatase (Schelbert *et al.*, 2009; Guyer *et al.*, 2014; Shimoda *et al.*, 2016), dephytilated by pheophytinase (Schelbert *et al.*, 2009) and the porphyrin ring of the resulting Pheide *a* is oxygenolytically cleaved by Pheide *a* oxygenase to yield colorless catabolites (Hörtensteiner, 2006). Although chloroplasts contain all the activities required for these reactions (Hörtensteiner, 2006, 2009; Schelbert *et al.*, 2009), the finding of Chlide *a* and Phein *a* in SAVs suggests that a fraction of leaf Chl might also be degraded in these vacuoles. Upon *in vitro* incubation of isolated SAVs, the levels of Chlide *a*, Phein *a* and Pheide *a* increase dramatically. This indicates that SAVs are competent to carry out the initial steps of the chlorophyll degradation pathway. So far, the full set of enzymes required for the degradation of chlorophyll to colorless catabolites have been localized to plastids; however, chlorophyll degradation enzymes might traffic from chloroplasts to SAVs to carry out Mg^{2+} dechelation and dephytylation. For example, chloroplast-targeted GFP (i.e. GFP fused to a chloroplast-targeting sequence) relocates to SAVs in senescing leaves of tobacco (Martínez *et al.*, 2008), raising the possibility that some Chl-degrading enzymes might also traffic from chloroplasts to SAVs. Thus, chloroplast-targeted Chl-degrading enzymes might provide part or all of the necessary machinery for the breakdown of PSI-bound Chl in SAVs (Figure 3).

Independent pathways for PSII and PSI degradation during senescence?

The data shown here suggest that proteins of PSI may be broken down in SAVs and rule out the participation of

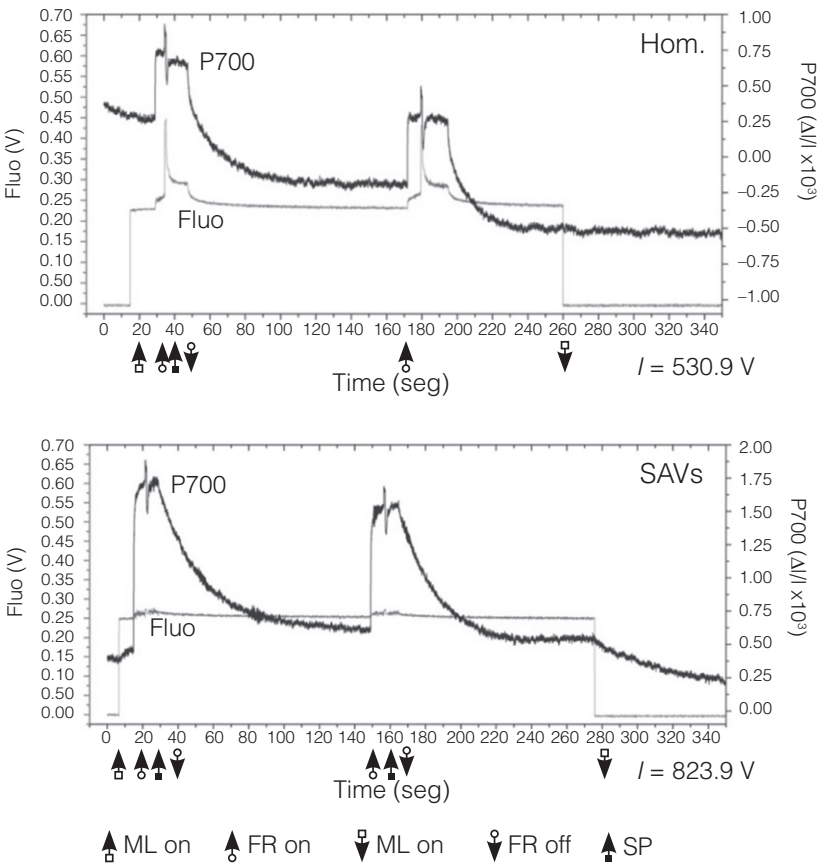

Figure 6. Modulated photosystem II (PSII) chlorophyll fluorescence (thin line) and light-induced absorbance changes of PSI at 830 nm (thick line) in the crude leaf homogenate (Hom, upper panel) and isolated 'senescence-associated vacuoles' (SAVs, lower panel) of leaves induced to senesce for 2 days in darkness. Assay mixtures contained 26 (leaf homogenate) and 39 (SAVs) μg Chl mL^{-1}. For the modulated chlorophyll fluorescence (PSII) assay, a pulse modulated measuring light (ML) was switched on at the start of the experiment. Saturating light pulses (SPs) were fired to reduce Q_A (the primary electron acceptor of PSII) and record the maximum fluorescence emission of PSII. For the redox kinetic assay of P700 (PSI), a far-red source (FR) was used to achieve the complete oxidation of PSI and record light-induced changes in P700 oxidation/reduction. On the right-hand side of the panels, the potential of the calibration detector is shown.

SAVs in the degradation of PSII proteins. There is evidence for the degradation of PSII proteins within the chloroplast by chloroplast-targeted proteases, and the degradation of PSII antenna components during senescence is partially dependent upon the activity of the chloroplastic *psbM* gene (Kohzuma *et al.*, 2017). Chloroplastic DegP and FtsH proteases seem to cooperate in D1 degradation during photoinhibition (Kapri-Pardes *et al.*, 2007; Sun *et al.*, 2007, 2010), and it seems likely that they might also be responsible for D1 degradation during senescence. FtsH11 is a chloroplast envelope protein possibly involved in altering the chloroplast import machinery; FtsH11 mutants show lower levels of PSI relative to PSII under long-day photoperiods in Arabidopsis (Wagner *et al.*, 2016); however, SAVs are devoid of FtsH11 (Figure 5). The hypothetical operation of separate pathways for PSII and PSI degradation might be consistent with previous physiological evidence. There are cases where PSI is lost ahead of PSII (e.g. Miersch *et al.*, 2000; Tang *et al.*, 2005; Moy *et al.*, 2015), or where PSII drops faster than PSI activity (Hilditch *et al.*, 1986), which might be consistent with the operation of two different pathways, possibly located in different cell compartments, for the degradation of each photosystem. An estimation of the proportion of SAVs with a clear Chl-fluorescence signal in senescing leaves of PSI- or PSII-less mutants of Arabidopsis (Meurer *et al.*, 1996), or in *stay green* mutants that specifically fail to break down certain components of the thylakoid membranes (*e.g. cytG* of soybeans; Guiamét *et al.*, 1991, 2002) may help to assess whether SAVs are specifically involved in the breakdown of Chl–protein complexes of PSI and associated pigment molecules during the senescence of leaves.

EXPERIMENTAL PROCEDURES

Plant material and growing conditions

Plants of tobacco (*N. tabacum* L. cv. Petit Havana) were grown in pots containing soil in naturally lit glasshouses, held at 20°C day/15°C night, in La Plata (Argentina, 34°55′S, 57°54′W) during March–November, or in Kiel (Germany, 54°20′N, 10°7′E) during August–October. In most experiments, mature leaves were detached, placed on moist filter paper in plastic boxes and induced to senesce in continuous darkness for 1–2 days at 20°C.

Isolation of SAVs

The isolation of SAVs was carried out as described by Martínez *et al.* (2008). Approximately 12 g of tobacco leaves were homogenized on ice in 50 mL of buffer [25 mM HEPES, pH 7.5, 0.6 M mannitol, 6.2 mM cysteine, 2 mM EDTA, 1% (w/v) polyvinylpolypyrrolidone (PVPP) and 1 mM phenylmethylsulfonyl fluoride (PMSF)]. To stain SAVs with the acidotropic marker Neutral Red, this homogenate was stirred gently for 15 min in the presence of 0.1 mg/mL Neutral Red, filtered through a nylon mesh and

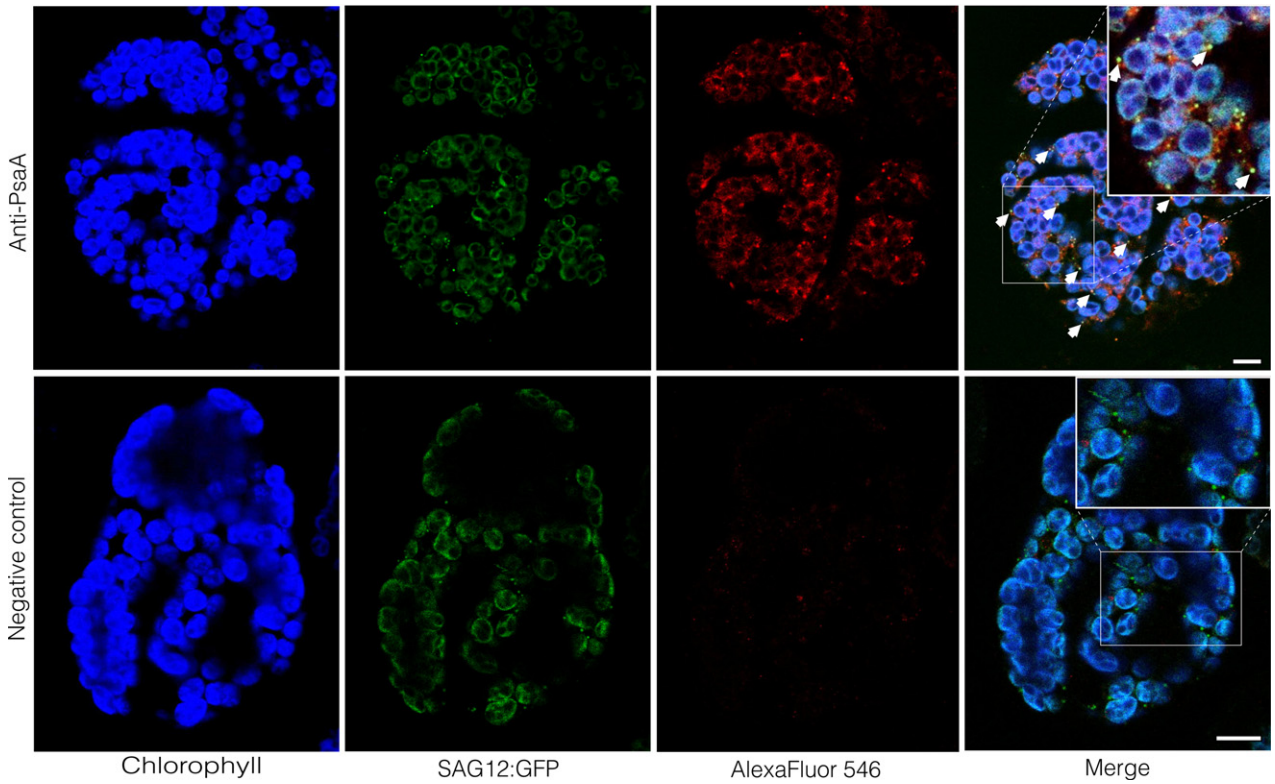

Figure 7. Immunolocalization of PsaA in 'senescence-associated vacuoles' (SAVs). Confocal microscopy images of isolated cells from senescing leaves (i.e. leaves incubated in darkness for 2 days) of an SAG12-GFP line of tobacco. From left to right, SAG12-GFP (488/510–540 nm, excitation/emission settings), anti-PsaA antibody detected with a secondary antibody coupled to Alexa Fluor (543/560–590 nm, excitation/emission settings) and merged image. The lower panel shows a representative cell from a negative control (primary antibody omitted). Part of the merged image is enlarged in the upper right corner. Scale bars: 5 μm. Arrows show representative SAVs detected through GFP fluorescence containing a strong PsaA signal. Note the absence of the 560–590 nm emission signal in the negative control.

centrifuged at 3500 ***g*** for 10 min at 4°C to pellet chloroplasts and chloroplast membranes. The supernatant was layered on top of a discontinuous sucrose gradient (5, 25, 35, 45 and 60% w/v sucrose prepared in 25 mM HEPES, pH 7.5, 0.6 M mannitol) and centrifuged at 100 000 ***g*** in a swinging bucket rotor for 1 h at 4°C in an Optima-Max Ultracentrifuge (Beckman-Coulter, https://www.beckman.com/). To remove externally contaminating soluble proteins, the fraction enriched in SAVs was treated with thermolysin (30 μg/mL) at 4°C for 20 min. Thermolysin treatment was terminated by adding EGTA to a final concentration of 0.16 mM, and SAVs were then re-isolated on a density gradient as described above. To stain SAVs with the specific substrate for cysteine proteases, R6502 (Rhodamine 110, *bis*-CBZ-L-phenylalanyl-L-arginine amide; Molecular Probes Inc., now ThermoFisher Scientific, https://www.thermofisher.com), after thermolysin treatment the first fraction enriched in SAVs was incubated at 30°C for 15 min with 200 μM R6502, and then re-isolated on a density gradient as described above.

Flow cytometry analysis of isolated SAVs

Isolated SAVs were diluted with phosphate buffer (50 mM, pH 7) and analysed with a flow cytometer (FACSCalibur; Becton Dickinson, https://www.bd.com) with excitation at 488 nm and fluorescence emission detection at 515–545 nm (R6502), 564–606 nm (Neutral Red) and >670 nm (chlorophyll). For each sample, 20 000 events were gated. Density plots were processed with FLOWING SOFTWARE 1.6 (Perttu Terho, Cell Imaging Core, Turku Centre for Biotechnology, Finland, http://www.flowingsoftware.com).

Chlorophyll, chlorophyllide, pheophytin and pheophorbide determination

Leaf Chl content was determined non-destructively with an SPAD 502 Chlorophyll Meter by averaging four or five measurements taken along the leaf main axis. An HPLC analysis was carried out to determine the pigment composition of SAVs. Isolated SAVs were diluted with an equal volume of buffer (HEPES 25 mM, pH 7.5, 0.6 M mannitol) and then centrifuged at 16 000 ***g*** for 25 min at 4°C. The SAV pellet was dissolved in acetone (80% v/v), buffered with HEPES 25 mM, pH 7.5, centrifuged at 16 000 ***g*** for 5 min, and the supernatant was recovered and filtered through a 0.22-μm nylon mesh before injection into an HPLC system. Samples were run in a Chromsep C18 column using a linear gradient in 15 min from 100% solvent A (80% methanol in 1 M ammonium acetate) to 100% solvent B (80% methanol in acetone). Solvent B was run until all pigments were completely eluted. The flow rate was 1 mL min^{-1}, and absorbance was detected at 667 nm. A Chl *a* standard was prepared from *Arthrospira* sp. as described by Iriyama *et al.* (1974). The Chl *b* standard was prepared by isolating chlorophyll from spinach leaves with the purification of Chl *b* in a sucrose chromatography column. Chlide *a* was prepared from Chl *a* using recombinant chlorophyllase (Benedetti and Arruda, 2002). Pheide *a* was prepared from Chlide *a* by acidification with hydrochloric acid. Phein *a* was prepared by acid treatment of Chl *a*. Figure S1 shows the retention times of these chlorophyll catabolite standards.

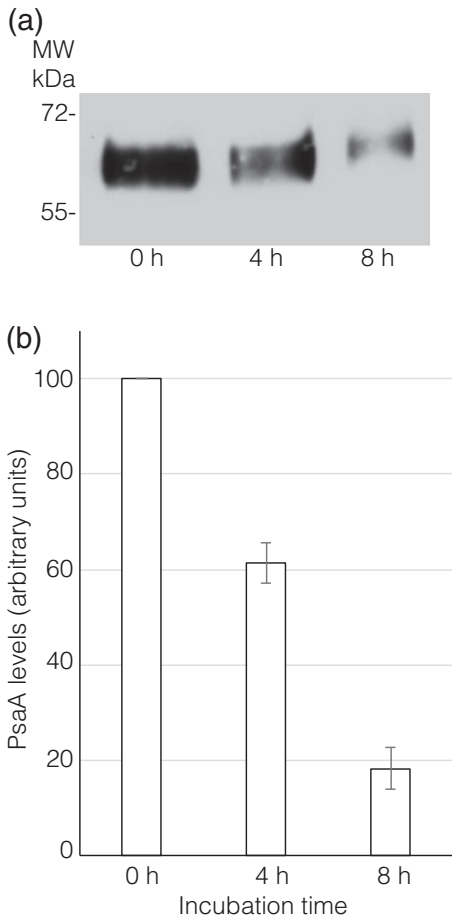

Figure 8. PsaA degradation in isolated 'senescence-associated vacuoles' (SAVs).
(a) SAVs were incubated at 30°C for 8 h. Equal aliquots of the SAV fraction were sampled at 0, 4 and 8 h of incubation and analyzed by Western blot using an antibody against PsaA.
(b) Quantitation of the changes in PsaA levels during the incubation of SAVs (PsaA levels expressed as a percentage of levels before incubation, quantitation based on data from three independent experiments, vertical bars show the standard error). The position of apparent molecular mass markers is shown on the left-hand side of the blot.

For the *in vitro* chlorophyll degradation assay, PMSF was omitted from the homogenization buffer, and isolated SAVs were incubated at 30°C for 6, 10 and 14 h in darkness prior to the HPLC analysis described above.

Chlorophyll fluorescence emission spectra and P700 determinations

Chlorophyll fluorescence emission spectra were determined with a Fluorescence Spectrophotometer (F-4500 FL; Hitachi, https://www.hitachi.com). The excitation wavelength was set at 440 nm (Mullet *et al.*, 1980) and spectra were recorded at a sampling interval of 2.0 nm. Dilutions of isolated SAVs and the crude extract from tobacco leaves were analysed first at room temperature and then at 77 K. The simultaneous measurement of P700 activity and PSII chlorophyll fluorescence was performed with a DUAL-PAM-100 (Heinz Walz GmbH, https://www.walz.com/). Isolated SAVs and the crude extract (from which SAVs were isolated) were diluted with buffer (HEPES 25 mM, pH 7.5, 0.6 M mannitol and 25% sucrose w/v) before measurement.

Non-denaturing gel electrophoresis and mass spectrometric protein analysis

Non-denaturing gel electrophoresis was carried out according to Sárvári and Nyitrai (1994). Thylakoids were isolated as described by Tambussi *et al.* (2000). The samples were solubilized in decyl-maltoside:heptyl-thioglucoside:SDS (4.5:4.5:1 w/w), in a ratio of Chl/detergent of 1:40 (w/w). An aliquot of solubilized sample corresponding to 14 μg of Chl was loaded into each well. The topmost green band was excised from the gel and analysed by tandem MS/MS spectrometry according to the method described by Kufryk *et al.* (2008).

Western blot analysis and autodigestion assays

Western blot analyses were carried out as described in Tambussi *et al.* (2000). A 7.5-μg portion of protein was loaded into each lane. Antibodies against PsaA and Lhca1–Lhca4 were purchased from Agrisera AB (https://www.agrisera.com). For autodigestion experiments, SAVs were isolated without protease inhibitors. SAVs were incubated in darkness at 30°C and PsaA levels were analysed by Western blotting before and after incubation. Blots from three independent experiments were scanned and band intensity was quantitated with IMAGEJ (https://imagej.nih.gov/ij/).

Immunofluorescence localization of PsaA in SAVs of isolated cells

For these experiments, a tobacco line expressing GFP fused to SAG-12 (Carrión *et al.*, 2013) was used. Leaves were cut into small (2 × 2 mm) pieces and infiltrated twice under vacuum (5 min each time) with 0.25% w/v Macerozyme dissolved in acetate buffer (25 mM, pH 5.5, 0.6 M mannitol). After 2 h of incubation at 37°C, cell debris and non-digested tissue were separated by filtration through a nylon mesh and isolated cells were collected by low-speed centrifugation (50 ***g***). Cells were washed twice with acetate buffer (25 mM, pH 5.5, 0.6 M mannitol) and fixed at 4°C for 2 h with 4% (w/v) paraformaldehyde, 0.6 M mannitol, in 25 mM 2-(*N*-morpholino) ethanesulfonic acid (MES) buffer, pH 7. After washing the cells twice with PBST (10 mM Na_2HPO_4, 1.8 mM KH_2PO_4, 137 mM NaCl plus 0.05% v/v Tween 20), they were incubated with anti-PsaA antibody (1:500 v/v in PBST, 1% w/v BSA) for at least 3 h at 4°C, then washed twice again with PBST. Cells were then incubated for 2 h with secondary antibody (goat anti-rabbit IgG conjugated to Alexa Fluor 546, diluted 1:200 v/v with PBST plus 1% w/v BSA), and washed twice with PBST before confocal microscopy observations. Negative controls were prepared by omitting the primary anti-PsaA antibody incubation. Settings for the confocal microscope were 488/510–540 nm (excitation/emission) for GFP, 543/560–590 nm (excitation/emission) for Alexa Fluor 546 and 488/>680 nm (excitation/emission) for chlorophyll autofluorescence. To quantitatively test the colocalization between SAG12:GFP and PsaA immunolabeled fluorescence signals, the PSC colocalization plug-in (French *et al.*, 2008) was used to estimate the linear Pearson and the non-linear Spearman's rank correlation coefficients (French *et al.*, 2008).

ACKNOWLEDGEMENTS

We thank Prof. W. Bilger and L. Nichelmann (Botanisches Institut, Christian-Albrechts-Universität zu Kiel) for their help with low-temperature fluorescence emission spectra and P700 measurements, and Dr F. Chirdo (Universidad Nacional de La Plata, Argentina) for

his help with flow cytometry. We also appreciate the suggestions and criticisms raised by two anonymous reviewers. This work was funded by FONCYT (Argentina) through PICT 0784, the Swedish Energy Agency (to C.F.) and Umeå University (to C.F.). F.M.G., M.L.C. and J.J.G. are researchers of CONICET (Argentina).

CONFLICT OF INTEREST

The authors declare no conflicts of interest.

SUPPORTING INFORMATION

Additional Supporting Information may be found in the online version of this article.

Figure S1. Typical chromatograms showing the retention times (minutes) of chlorophyll and chlorophyll catabolite standards.

REFERENCES

Allen, K.D. and Staehelin, L.A. (1991) Resolution of 16-20 chlorophyll-protein complexes using a low ionic strength native green gel system. *Anal. Biochem.* **194**, 214–222.

Benedetti, C.E. and Arruda, P. (2002) Altering the expression of the chlorophyllase gene ATHCOR1 in transgenic Arabidopsis caused changes in the Chlorophyll-to-Chlorophyllide ratio. *Plant Physiol.* **128**, 1255–1263.

Carrión, C.A., Costa, M.L., Martínez, D.E., Mohr, C., Humbeck, K. and Guiamet, J.J. (2013) *In vivo* inhibition of cysteine proteases provides evidence for the involvement of 'senescence-associated vacuoles' in chloroplast protein degradation during dark-induced senescence of tobacco leaves. *J. Exp. Bot.* **64**, 4967–4980.

Carrión, C.A., Martínez, D.E., Costa, M.L. and Guiamet, J.J. (2014) Senescence-associated vacuoles, a specific lytic compartment for degradation of chloroplasts proteins? *Plants*, **3**, 498–512.

Chiba, A., Ishida, H., Nishizawa, N.K., Makino, A. and Mae, T. (2003) Exclusion of ribulose-1,5-bisphosphate carboxylase/oxygenase from chloroplasts by specific bodies in naturally senescing leaves of wheat. *Plant Cell Physiol.* **44**, 914–921.

Dettmer, J., Hong-Hermesdorf, A., Stierhof, Y.-D. and Schumacher, K. (2006) Vacuolar H^+-ATPase activity is required for endocytic and secretory trafficking in Arabidopsis. *Plant Cell*, **18**, 715–730.

French, A.P., Mills, S., Swarup, R., Bennett, M.J. and Pridmore, T.P. (2008) Colocalization of fluorescent markers in confocal microscope images of plant cells. *Nat. Protoc.* **3**, 619–628.

Govindjee, G. (2004) Chlorophyll *a* fluorescence: a bit of basics and history. In *Chlorophyll a* Fluorescence (Papageorgiou, G. C. and Govindjee, G., eds). Dordrecht: The Netherlands: Springer, pp. 1–41.

Guiamét, J.J., Schwartz, E., Pichersky, E. and Noodén, L.D. (1991) Characterization of cytoplasmic and nuclear mutations affecting chlorophyll and chlorophyll-binding proteins during senescence in soybean. *Plant Physiol.* **96**, 227–231.

Guiamét, J.J., Tyystjärvi, E., Tyystjärvi, T., John, I., Kairavuo, M., Pichersky, E. and Noodén, L.D. (2002) Photoinhibition and loss of photosystem II reaction center proteins during senescence of soybean leaves. Enhancement of photoinhibition by the "stay-green" mutation *cytG*. *Physiol. Plant.* **115**, 468–478.

Guyer, L., Schelbert Hofstetter, S., Christ, B., Lira, B.S., Rossi, M. and Hörtensteiner, S. (2014) Different mechanisms are responsible for chlorophyll dephytylation during fruit ripening and leaf senescence in tomato. *Plant Physiol.* **166**, 44–56.

Hilditch, P., Thomas, H. and Rogers, L. (1986) Leaf senescence in a non-yellowing mutant of Festuca pratensis: photosynthesis and photosynthetic electron transport. *Planta*, **167**, 146–151.

Hinder, B., Schellenberg, M., Rodoni, S., Ginsburg, S., Vogt, E., Martinoia, E., Matile, P. and Hörtensteiner, S. (1996) How plants dispose of chlorophyll catabolites. Directly energized uptake of tetrapyrrolic breakdown products into isolated vacuoles. *J. Biol. Chem.* **271**, 27233–27236.

Hörtensteiner, S. (2006) Chlorophyll degradation during senescence. *Annu. Rev. Plant Biol.* **57**, 55–77.

Hörtensteiner, S. (2009) Stay-green regulates chlorophyll and chlorophyll-binding protein degradation during senescence. *Trends Plant Sci.* **14**, 155–162.

Hu, X., Makita, S., Schelbert, S., Sano, S., Ochiai, S., Tsuchiya, T., Hasegawa, S.F., Hörtensteiner, S., Tanaka, A. and Tanaka, R. (2015) Reexamination of chlorophyllase function implies its involvement in defense against chewing herbivores. *Plant Physiol.* **167**, 660–670.

Iriyama, K., Ogura, N. and Takamiya, A. (1974) A simple method for extraction and partial purification of chlorophyll from plant material, using dioxane. *J. Biochem.* **76**, 901–904.

Ishida, H., Yoshimoto, K., Izumi, M., Reisen, D., Yano, Y., Makino, A., Ohsumi, Y., Hanson, M.R. and Mae, T. (2008) Mobilization of Rubisco and stroma-localized fluorescent proteins of chloroplast to the vacuole by an ATG gene-dependent autophagic process. *Plant Physiol.* **148**, 142–155.

Kapri-Pardes, E., Naveh, L. and Adam, Z. (2007) The thylakoid lumen protease DegP1 is involved in the repair of photosystem II from photoinhibition in Arabidopsis. *Plant Cell*, **19**, 1039–1047.

Kariola, T., Brader, G., Li, J. and Palva, E.T. (2005) Chlorophyllase 1, a damage control enzyme, affects the balance between defense pathways in plants. *Plant Cell*, **17**, 282–294.

Kohzuma, K., Sato, Y., Ito, H. *et al.* (2017) The non-Mendelian green cotyledon gene in soybean encodes a small subunit of photosystem II. *Plant Physiol.* **173**, 2138–2147.

Krupinska, K. (2007) Fate and activities of plastids during leaf senescence. In *The Structure and Function of Plastids*. (Wise, R. R. and Hoober, J. K., eds). NL: Springer, pp. 433–449.

Kuai, B., Chen, J. and Hörtensteiner, S. (2018) The biochemistry and molecular biology of chlorophyll breakdown. *J. Exp. Bot.* **69**, 751–767.

Kufryk, G., Hernandez-Prieto, M., Kieselbach, T., Miranda, H., Vermaas, W. and Funk, C. (2008) Association of small CAB-like proteins (SCP) of *Synechocystis* sp. PCC 6803 with Photosystem II. *Photosynth. Res.* **95**, 135–145.

Li, Z., Wu, S., Chen, J., Wang, X., Gao, J., Ren, G. and Kuai, B. (2017) NYEs/SGRs-mediated chlorophyll degradation is critical for detoxification during seed maturation in Arabidopsis. *Plant J.* **92**, 650–651.

Lin, Y.-P., Lee, T. Y., and Charng, Y. Y. (2014) Analysis of an Arabidopsis heat-sensitive mutant reveals that chlorophyll synthase is involved in reutilization of chlorophyllide during chlorophyll turnover. *Plant J.* **80**, 14–26.

Lin, Y.-P., Wu, M.-C. and Charng, Y. (2016) Identification of a chlorophyll dephytylase involved in chlorophyll turnover in Arabidopsis. *Plant Cell*, **28**, 2974–2990.

Mach, J.M., Castillo, A.R., Hoogstraten, R. and Greenberg, J.T. (2001) The *Arabidopsis*-accelerated cell death gene *ACD2* encodes red chlorophyll catabolite reductase and suppresses the spread of disease symptoms. *Proc. Natl. Acad. Sci. USA*, **98**, 771–776.

Martínez, D.E., Costa, M.L., Gomez, F.M., Otegui, M.S. and Guiamet, J.J. (2008) "Senescence-associated vacuoles" are involved in the degradation of chloroplast proteins in tobacco leaves. *Plant J.* **56**, 196–206.

Meguro, M., Ito, H., Takabayashi, A., Tanaka, R. and Tanaka, A. (2011) Identification of the 7-hydroxymethyl chlorophyll *a* reductase of the chlorophyll cycle in *Arabidopsis*. *Plant Cell*, **23**, 3443–3453.

Meurer, J., Meierhoff, K. and Westhoff, P. (1996) Isolation of high-chlorophyll-fluorescence mutants of Arabidopsis thaliana and their characterisation by spectroscopy, immunoblotting and Northern hybridisation. *Planta*, **198**, 385–396.

Michaeli, S., Honig, A., Levanony, H., Peled-Zehavy, H. and Galili, G. (2014) Arabidopsis ATG8-Interacting Protein1 is involved in autophagy-dependent vesicular trafficking of plastid proteins to the vacuole. *Plant Cell*, **26**, 4084–4101.

Miersch, I., Heise, J., Zelmer, I. and Humbeck, K. (2000) Differential degradation of the photosynthetic apparatus during leaf senescence in barley (*Hordeum vulgare* L.). *Plant Biol.* **2**, 618–623.

Moy, A., Le, S. and Verhoeven, A. (2015) Different strategies for photoprotection during autumn senescence in maple and oak. *Physiol. Plant.*, **155**, 205–216.

Mullet, J.E., Burke, J.J. and Arntzen, C.J. (1980) Chlorophyll proteins of photosystem I. *Plant Physiol.* **65**, 814–822.

Otegui, M., Noh, Y.S., Martinez, D.E., Vila Petroff, M.G., Staehelin, L.A., Amasino, R. and Guiamét, J.J. (2005) Senescence-associated vacuoles

with intense proteolytic activity develop in leaves of Arabidopsis and soybean. *Plant J.* **41**, 831–844.

Ougham, H., Hörtensteiner, S., Armstead, I., Donnison, I., King, I., Thomas, H. and Mur, L. (2008) The control of chlorophyll catabolism and the status of yellowing as a biomarker of leaf senescence. *Plant Biol.* **10**, 4–14.

Preiss, S., Peter, G.F., Anandan, S. and Thornber, J.P. (1993) The multiple pigment-proteins of photosystem I antenna. *Photochem. Photobiol.* **57**, 152–157.

Pruzinska, A., Tanner, G., Anders, I., Roca, M. and Hörtensteiner, S. (2003) Chlorophyll degradation: pheophorbide a oxygenase is a Rieske-type iron-sulfur protein, encoded by the accelerated cell death 1 gene. *Proc. Natl. Acad. Sci. USA*, **100**, 15259–15263.

Sárvári, E. and Nyitrai, P. (1994) Separation of chlorophyll-protein complexes by deriphat polyacrylamide gradient gel electrophoresis. *Electrophoresis*, **15**, 1068–1071.

Sato, Y., Morita, R., Katsuma, S., Nishimura, M., Tanaka, A. and Kusaba, M. (2009) Two short-chain dehydrogenase/reductases, NON-YELLOW COLORING 1 and NYC1-LIKE, are required for chlorophyll b and light-harvesting complex II degradation during senescence in rice. *Plant J.* **57**, 120–131.

Scheer, H. (2006) An overview of chlorophylls and bacteriochlorophylls: biochemistry, biophysics, functions and applications. In *Chlorophylls and Bacteriochlorophylls: Biochemistry, Biophysics, Functions and Applications* (Grimm, B., Porra, R. J, Rüdiger, W. and Scheer, H., eds). Dordrecht, The Netherlands: Springer Netherlands, pp. 1–26.

Schelbert, S., Aubry, S., Borla, B., Agne, B., Kessler, F., Krupinska, K. and Hörtensteiner, S. (2009) Pheophytin pheophorbide hydrolase (pheophytinase) is involved in chlorophyll breakdown during leaf senescence in Arabidopsis. *Plant Cell*, **21**, 767–785.

Schenk, N., Schelbert, S., Kanwischer, M., Goldschmidt, E.E., Dörmann, P. and Hörtensteiner, S. (2007) The chlorophyllases AtCHL1 and AtCHL2 are not essential for senescence-related chlorophyll breakdown in *Arabidopsis thaliana*. *FEBS Lett.* **581**, 5517–5525.

Scheumann, V., Schoch, S. and Rüdiger, W. (1999) Chlorophyll *b* reduction during senescence of barley seedlings. *Planta*, **209**, 364–370.

Schreiber, U. (2004) Pulse-amplitude-modulation (PAM) fluorometry and saturation pulse method: an overview. In *Chlorophyll a* Fluorescence (Papageorgiou, G. C. and Govindjee, G., eds). Dordrecht, The Netherlands: Springer Netherlands, pp. 279–319.

Shimoda, Y., Ito, H. and Tanaka, A. (2016) Arabidopsis *STAY-GREEN*, Mendel's green cotyledon gene, encodes Magnesium-dechelatase. *Plant Cell*, **28**, 2147–2160.

Sims, D.A. and Gamon, J.A. (2002) Relationships between leaf pigment content and spectral reflectance across a wide range of species, leaf structures and developmental stages. *Remote Sens. Environ.* **81**, 337–354.

Sun, X., Peng, L., Guo, J., Chi, W., Ma, J., Lu, C. and Zhang, L. (2007) Formation of Deg5 and Deg8 complexes and their involvement in the degradation of photodamaged photosystem II reaction center D1 protein in Arabidopsis. *Plant Cell*, **19**, 1347–1361.

Sun, X., Fu, T., Chen, N., Guo, J., Ma, J., Zou, M., Lu, C. and Zhang, L. (2010) The stromal chloroplast Deg7 protease participates in the repair of photosystem II after photoinhibition in Arabidopsis. *Plant Physiol.* **152**, 1263–1273.

Tambussi, E.A., Bartoli, C.G., Beltrano, J., Guiamet, J.J. and Araus, J.L. (2000) Oxidative damage to thylakoid proteins in water-stressed leaves of wheat (*Triticum aestivum*). *Physiol. Plant.*, **108**, 398–404.

Tang, Y., Wen, X. and Lu, C. (2005) Differential changes in degradation of chlorophyll-protein complexes of photosystem I and photosystem II during flag leaf senescence of rice. *Plant Physiol. Biochem.* **43**, 193–201.

Wada, S., Ishida, H., Izumi, M., Yoshimoto, K., Ohsumi, Y., Mae, T. and Makino, A. (2009) Autophagy plays a role in chloroplast degradation during senescence in individually darkened leaves. *Plant Physiol.* **149**, 885–893.

Wagner, R., von Sydow, L., Aigner, H., Netotea, S., Brugière, S., Sjögren, L., Ferro, M., Clarke, A. and Funk, C. (2016) Deletion of FtsH11 protease has impact on chloroplast structure and function in Arabidopsis thaliana when grown under continuous light. *Plant, Cell Environ.* **39**, 2530–2544.

Wang, S. and Blumwald, E. (2014) Stress-induced chloroplast degradation in Arabidopsis is regulated through a process independent of autophagy and senescence-associated vacuoles. *Plant Cell*, **26**, 4875–4888.